The mineralocorticoid receptor plays a transient role in mouse skin development

Julia Boix[1], Elena Carceller[1], Lisa M. Sevilla[1], Víctor Marcos-Garcés[1], Paloma Pérez[1*]

[1]Instituto de Biomedicina de Valencia, Consejo Superior de Investigaciones Científicas (IBV-CSIC)

*** Corresponding author**: Paloma Pérez, IBV-CSIC, Jaime Roig 11, E-46010-Valencia, Spain.
Tel +34 96 339 1766
Fax +34 96 369 0800
pperez@ibv.csic.es

Short title: MR function in skin development

Keywords: Mineralocorticoid receptor, skin, epidermis, keratinocyte, development, glucocorticoid receptor

Word count: 1099

Funding
This work was supported by the Spanish Ministerio de Ciencia e Innovación (grant SAF2011-28115).

Abstract

Glucocorticoid (GC) hormones can bind two structurally and functionally related steroid receptors: the GC Receptor (GR or *Nr3c1*) and the mineralocorticoid receptor (MR or *Nr3c2*), which recognize the same DNA response elements and act as ligand-dependent transcription factors. While the crucial role of GR for skin homeostasis has been widely characterized, the exact role of MR in this tissue deserves further study. We assessed NR3C2 expression in developing and adult WT mouse skin and found a transient peak at embryonic day (E)16.5, which along with low levels of HSD11B2, the enzyme inactivating GCs, supports a role for GC-MR complexes in epidermal maturation. Consistent with this observation, $MR^{-/-}$ embryonic skin showed alterations in early epidermal differentiation that resolved postnatally. The lack of a more severe skin phenotype of $MR^{-/-}$ mice suggests functional compensation by GR in this tissue in the perinatal period.

Background

The importance of hormonal regulation in skin is evidenced by numerous endocrine abnormalities with cutaneous manifestations, including disorders of the epidermal barrier and hair (1, s1). Hormone action is mediated by nuclear receptor superfamily members, ligand-activated transcription factors that integrate multiple cellular processes, including the glucocorticoid (GC) receptor (GR or *Nr3c1*) and the mineralocorticoid receptor (MR or *Nr3c2*) (2). Both proteins are structurally and functionally related, and upon GC binding recognize the same hormone responsive elements to transcriptionally regulate target genes (3-5). GC access to GR and MR is modulated by two enzymes, 11β-hydroxy steroid dehydrogenases type I and II (HSD11B1/HSD11B2), which mediate interconversion between inactive and active GCs. Human and mouse skin can synthesize GCs and key enzymes of steroid synthesis, acting as a functional hypothalamo-pituitary-adrenal axis to secure epidermal homeostasis (6, s2, s3). While our previous work demonstrated that GR is required for epidermal development and homeostasis (7, 8, s4), much less is known regarding MR in this tissue (9). Remarkably, transgenic mice with keratinocyte-specific overexpression of either MR or GR (s5, s6) showed strong phenotypical similarities at birth including atrophic skin, reduced hair follicle number, and impaired epidermal maturation.

Questions addressed

We have analyzed: i) MR expression during mouse skin development; ii) the consequences of MR inactivation in developing mouse skin; and iii) the relative expression of HSD11B1/HSD11B2 during this process.

Experimental design

Animal Experimentation

$MR^{-/-}$ mice were generated using generalized CRE-mediated recombination by intercrossing K5-cre mice (s7) and $MR^{loxP/loxP}$ mice (s8).

Sample processing

Skin samples were collected from at least three individuals of each genotype and age and analyzed as reported (8). Mean value ± SD was calculated and statistical significance assessed using the Student's t-test (8).

Results

We analyzed the relative expression of *Nr3c2* by RT-QPCR in WT embryonic (E)18.5 and adult mouse skin in the telogen (8-wk old) and anagen (5-wk old) phases of the hair cycle. *Nr3c2* levels were 17-fold higher in telogen relative to anagen skin, suggesting a role for MR in the resting phase of the hair cycle; however, *Nr3c2* was most abundant in E18.5 skin, 5-fold higher than in telogen adult skin (Fig. 1A). Assessment of *Nr3c2* during skin development revealed a peak in expression at E16.5 which decreased thereafter (E18.5 and postnatal day 0 (P0); Fig. 1B). These findings were paralleled by changes in MR protein expression in developing and adult skin (Fig. 1C). *Nr3c1* levels also peaked in E16.5 skin but unlike *Nr3c2* did not decrease at later timepoints (Fig. S1). *Krt77* and *Sprr2d* are controls known to be expressed differentially during epidermal development (Fig. S1).

To evaluate the consequences of MR loss-of-function in developing skin, we generated $MR^{-/-}$ mice (Fig. 1D) using generalized CRE-mediated recombination in $MR^{loxP/loxP}$ mice (Supp. Information; s7, s8). $MR^{-/-}$ mice died perinatally around P10 similar to $MR^{null/null}$ mice (s9), presumably due to renal loss of sodium and water (not shown). Epidermal permeability assays in $MR^{+/-}$ and $MR^{-/-}$ E17.5 embryos showed no major changes in the pattern of barrier formation among genotypes (Fig. 1E). However, analysis of Hematoxylin/Eosin stained skin sections showed statistically significant increases of epidermal thickness in $MR^{-/-}$ relative to $MR^{+/-}$ embryos (Fig. 1E, F). Altered differentiation, with a more restricted expression of keratin (K)5 and abnormal expression patterns of K10 and loricrin (LOR) were also detected in $MR^{-/-}$ embryos and quantitated as minor but statistically significant changes of percent positive layers (Fig. 1E, G). These alterations resolved spontaneously with age as $MR^{-/-}$ skin had a similar

appearance as $MR^{+/-}$ or WT littermates at P0 and P4 (Fig. 2 and data not shown). We assessed stratum corneum lipids by Nile red staining and quantitated epidermal thickness and loricrin staining in postnatal skin samples but found no changes among genotypes (Fig. 2A and S2). $MR^{-/-}$ epidermal proliferation was unchanged at P0 but statistically significant increases were detected at P4 (Fig. 2B), relative to controls; however, we cannot exclude the possibility that the $MR^{-/-}$ postnatal renal defects indirectly affect proliferation in this tissue.

To understand whether the transient role of MR in epidermal development is due to alterations in GC availability, we assessed *Hsd11b1* and *Hsd11b2* in skin at distinct stages and observed pronounced peaks in expression for both genes at E18.5 (Fig. 2C). In adult skin, the expression of *Hsd11b1* decreased 2-fold and that of *Hsd11b2* more than 30-fold relative to E18.5. Immunostaining confirmed the restricted expression of HSD11B2 to the upper epidermal layers with statistically significant increases at P0 (Fig. 2D and S3A). Importantly, HSD11B2 epidermal expression was similar in $MR^{+/+}$ *vs* $MR^{-/-}$ mice but decreased significantly in $GR^{-/-}$ skin (Fig. 2E and S3B).

The α-subunit of the amiloride-sensitive epithelial Na channel (*ENaCα*/*Scnn1a*), necessary for epidermal homeostasis, is a transcriptional target of both MR and GR (s10). We assessed whether the absence of MR affected *ENaCα* but found no differences in P0 skin (Fig. S4), similar to that reported in colon and kidney of $MR^{-/-}$ newborn mice (s11). The fact that *Nr3c1* levels are unchanged in $MR^{-/-}$ skin suggests that GR expression is not negatively affected by loss of MR (Fig. S4).

Conclusions

Our findings indicate that MR plays a role in regulating epidermal differentiation at late embryonic stages. The transient expression peak of MR at E16.5, coinciding with low levels of HSD11B2, argues for a role of GC-MR complexes in epidermal maturation. The fact that HSD11B2 was virtually absent in $GR^{-/-}$ skin but normally expressed in $MR^{-/-}$ skin, together with its reported induction by dexamethasone in human keratinocytes (s12), suggests this enzyme is regulated by GR but not MR, and may represent a mechanism to modulate GC-dependent actions locally. The hypothalamo-pituitary-adrenal axis becomes active around E15.5 ensuring proper control of circulating GC and aldosterone levels, which are normally high perinatally (s13). MR and GR expression peaks shortly afterwards, at E16.5. MR expression decreases at later developmental timepoints while that for GR remains constant. This observation together with our phenotypic data supports the hypothesis that MR plays a transient role in skin development. While $GR^{-/-}$ late embryos featured defective epidermal differentiation with virtually absent stratum corneum and impaired barrier function (s4), the skin phenotype of $MR^{-/-}$ embryos was relatively milder suggesting functional compensation by GR in the perinatal period.

Acknowledgements

We thank Jose Nieto for expert technical help. JB, EC, and VMG are recipients of FPI, FPU (MINECO), and JAE-INTRO- CSIC fellowships. We thank COST ADMIRE BM-1301 for support for dissemination. JB generated the mouse model; JB, EC, LMS and VMG analyzed skin samples. PP designed the experiments and wrote the paper. All authors read and approved the manuscript.

Conflict of interest

The authors have declared no conflict of interests.

References

1 Slominski AT, Zmijewski MA, Skobowiat C, Zbytek B, Slominski RM & Steketee JD 2012 Sensing the environment: regulation of local and global homeostasis by the skin's neuroendocrine system. *Adv Anat Embryol Cell Biol* **212**:1–115.

2 Evans RM & Mangelsdorf DJ 2014 Nuclear Receptors, RXR, and the Big Bang. *Cell* **157**(1):255–266.
3 Oakley RH & Cidlowski JA 2013 The biology of the glucocorticoid receptor: new signaling mechanisms in health and disease. *J Allergy Clin Immunol* **132**(5):1033–44.
4 Funder JW 2010 Minireview: Aldosterone and Mineralocorticoid Receptors: Past, Present, and Future. *Endocrinology* **151**(11):5098–5102.
5 Martinerie L, Munier M, Menuet DL, Meduri G, Viengchareun S & Lombès M 2013 The mineralocorticoid signaling pathway throughout development: Expression, regulation and pathophysiological implications. *Biochimie* **95**:148–157.
6 Slominski AT, Manna PR & and Tuckey RC 2014 Cutaneous glucocorticosteroidogenesis: securing local homeostasis and the skin integrity *Experimental Dermatol*ogy **23**:369–374.
7 Pérez P 2011 Glucocorticoid receptors, epidermal homeostasis and hair follicle differentiation *Dermato-Endocrinology* Rewiew for the special issue of the Journal Nuclear Hormone Receptors **3**(3):1–9.
8 Sevilla LM, Latorre V, Sanchis A & Pérez P 2013 Epidermal inactivation of the glucocorticoid receptor triggers skin barrier defects and cutaneous inflammation. *Journal of Investigative Dermatology* **33**(2):361–370.
9 Farman N, Maubec E, Poeggeler B, Klatte JE, Jaisser F& Paus R 2010 The mineralocorticoid receptor as a novel player in skin biology:beyond the renal horizon? *Experimental Dermatol*ogy **19**:100–107.

Figure Legends

Fig. 1. MR expression in WT developing and adult mouse skin (A-C), and epidermal barrier formation and skin architecture in $MR^{-/-}$ mice (D-G). A. RT-QPCR data showing relative *Nr3c2* mRNA levels in WT developing (embryonic E18.5) and telogen and anagen adult mouse skin. Asterisks indicate statistically significant differences relative to E18.5. (n= 3 per age; * p-value <0.05; *** p-value <0.001). B. Relative *Nr3c2* mRNA levels in embryonic (E15.5-E18.5) and newborn (P0) mouse skin. Asterisks indicate statistically significant differences relative to E15.5 (n= 4 per age; *** p-value <0.001). C. Western blot showing MR protein in developing (E16.5, E18.5, P0) and adult mouse skin (8-wk old). Kidney whole cell extracts from $MR^{-/-}$ P0 or WT adult (K) demonstrate the specificity of the MR antibody. Actin is used as a loading control. D. *Nr3c2* transcript levels were assessed in $MR^{+/+}$, $MR^{+/-}$, and $MR^{-/-}$ P0 skin. Asterisks indicate statistically significant differences relative to $MR^{+/+}$ (n= at least 3 per genotype; ** p-value <0.01; *** p-value <0.001). E. Left panels: Epidermal permeability was assessed in E17.5 $MR^{+/-}$ and $MR^{-/-}$ mice (n=22) by toluidine blue staining. Blue denotes immature epidermis and white indicates mature epidermis. Right panels: Histological analysis. H&E indicates hematoxylin/eosin staining. Brackets illustrate differences in epidermal thickness, which were quantitated in panel F; asterisks indicate altered epidermal differentiation. Bar: 100 μm. F-G. Morphometric quantitation of epidermal thickness (F) and immunohistochemistry (G). Percentage of K5-, K10-, and loricrin (LOR)-positive layers is shown in G. Asterisks indicate statistically significant differences relative to $MR^{+/-}$ (n= 7 per genotype; * $p<0.05$, ** $p<0.01$, *** $p<0.001$).

Fig. 2. Skin architecture of postnatal $MR^{-/-}$ mice, and HSD11B2 expression during skin development. A. Hematoxylin/eosin (H&E) staining, immunolocalization of loricrin (LOR), and lipid distribution (Nile red staining) were examined in skin sections collected from $MR^{+/-}$ and $MR^{-/-}$ mice at P0 and P4. B. Epidermal proliferation was assessed in $MR^{+/-}$ and $MR^{-/-}$ P0 skin by *in vivo* BrdU incorporation. Statistically significant changes among genotypes were detected only at P4 (n= 6 per genotype; ** p-value <0.01). C. *Hsd11b1* and *Hsd11b2* mRNA levels were assessed in developing (E16.5, E18.5, P0) and adult mouse skin by RT-QPCR. Asterisks indicate statistically significant differences relative to E16.5 (n=3 per age; * p-value < 0.05; ** p-value < 0.01). D-E. Immunohistochemistry for HSD11B2 in skin sections from E16.5, E18.5 and P0 WT mice (n=12), as well as in P0 $MR^{+/+}$, $MR^{-/-}$ and $GR^{-/-}$ skin (n=12). Bars: 100 μm.

Boix, Fig. 1
A
Relative Nr3c2 mRNA levels
120
100
80
60
40
20
0
*
***
E18.5
Telogen
Anagen
B
Relative Nr3c2 mRNA levels
400
300
200
100
0
***
**
E15.5
E16.5
E18.5
P0
C
E16.5
E18.5
P0
Adult
MR-/- K
MR
Actin
D
Relative Nr3c2 mRNA levels
120
100
80
60
40
20
0
*
***
MR+/+
MR+/-
MR-/-
E
MR+/- E17.5
H&E
K5
K10
LOR
MR-/- E17.5
H&E
K5
K10
LOR
F
Epidermal thickness (μm)
120
80
40
0
***
MR+/-
MR-/-
G
Percentage of positive layers
100
80
60
40
20
0
MR+/-
MR-/-
**
*
*
K5
K10
LOR

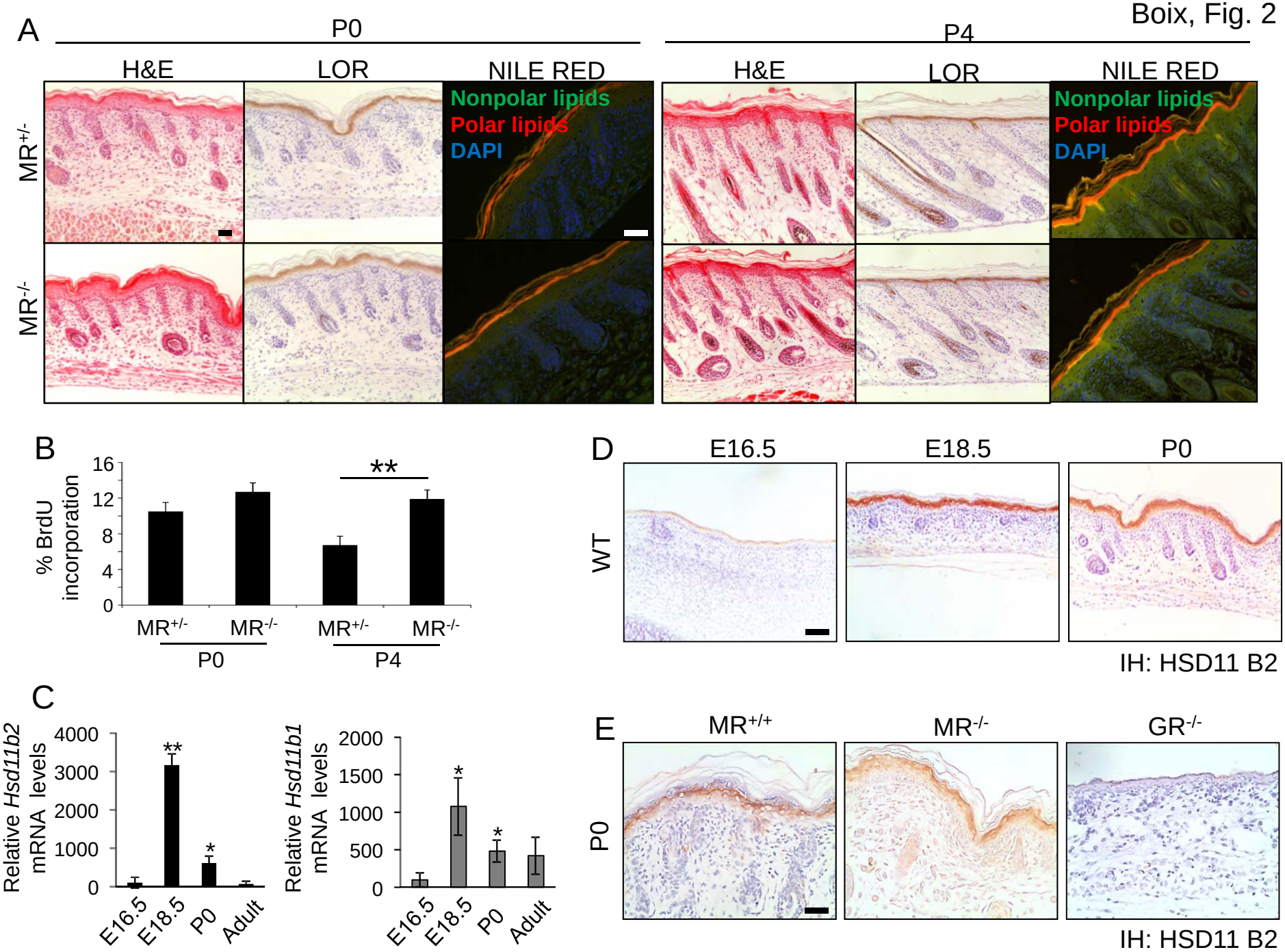
A
P0
P4
H&E
LOR
NILE RED
H&E
LOR
NILE RED
Nonpolar lipids
Polar lipids
DAPI
Nonpolar lipids
Polar lipids
DAPI
MR+/-
MR-/-
B
% BrdU incorporation
16
12
8
4
0
**
MR+/-
MR-/-
MR+/-
MR-/-
P0
P4
C
Relative Hsd11b2 mRNA levels
4000
3000
2000
1000
0
**
*
E16.5
E18.5
P0
Adult
Relative Hsd11b1 mRNA levels
2000
1500
1000
500
0
*
*
E16.5
E18.5
P0
Adult
D
E16.5
E18.5
P0
WT
IH: HSD11 B2
E
MR+/+
MR-/-
GR-/-
P0
IH: HSD11 B2

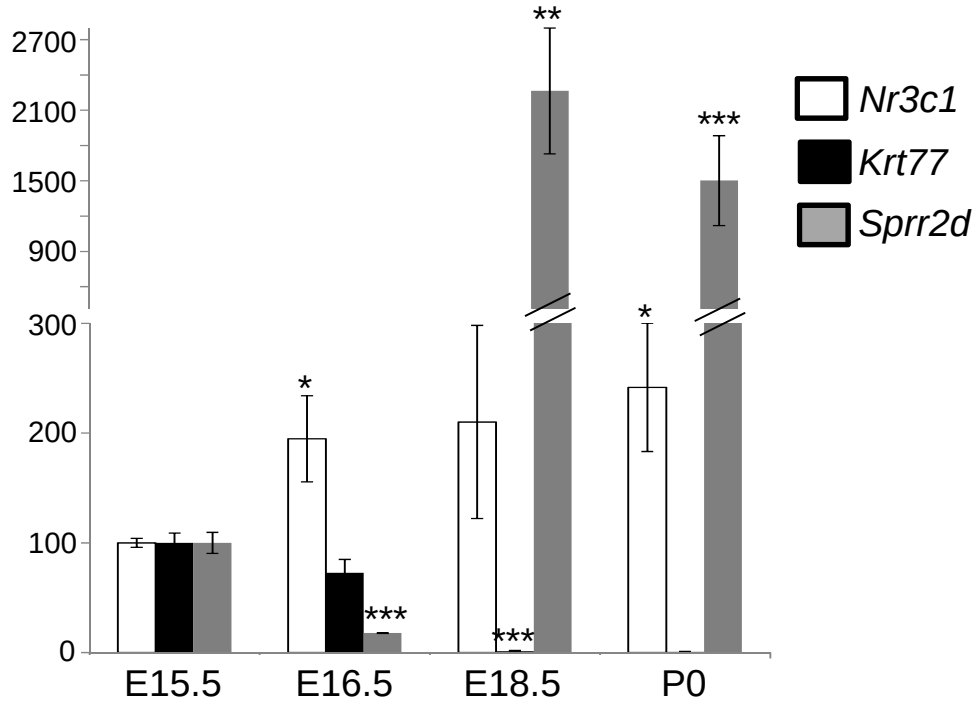
2700
2100
1500
900
300
200
100
0
E15.5
E16.5
E18.5
P0
*
**
***
***
*
***
Nr3c1
Krt77
Sprr2d

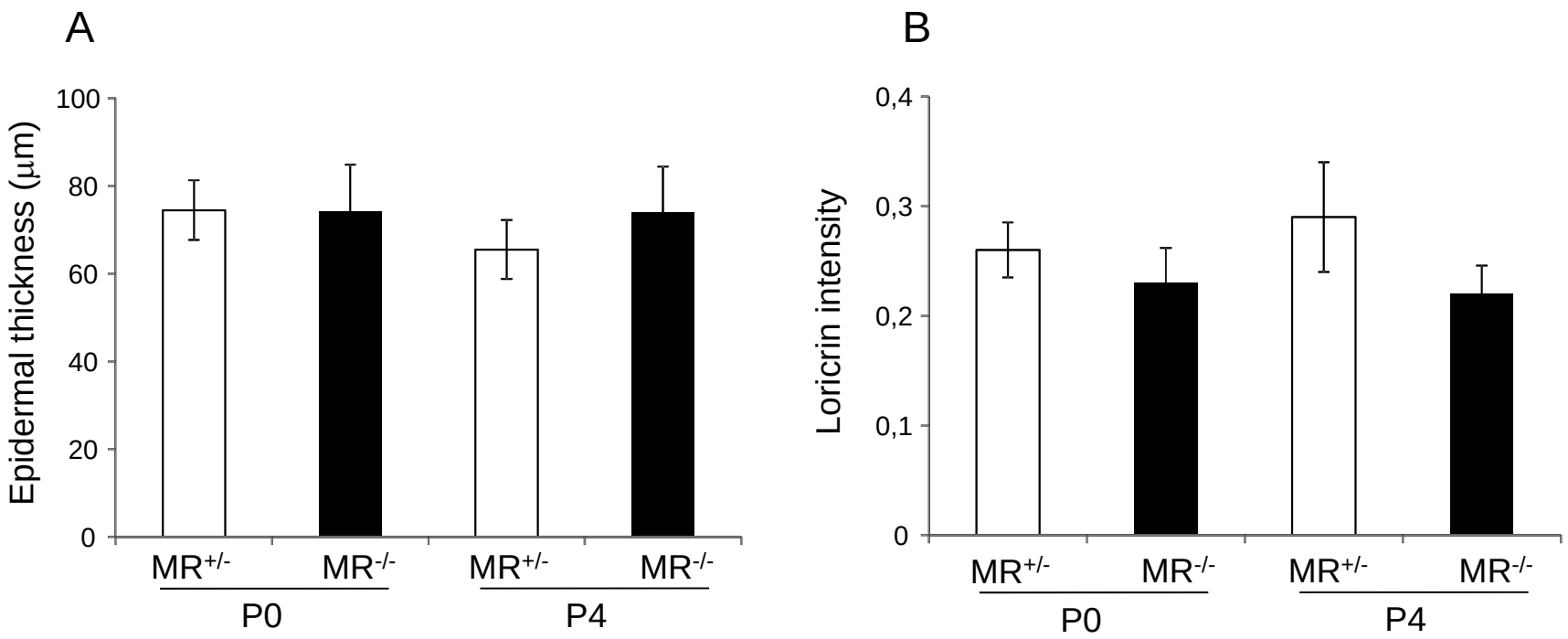
A
Epidermal thickness (µm)
100
80
60
40
20
0
MR+/-
MR-/-
MR+/-
MR-/-
P0
P4
B
Loricrin intensity
0,4
0,3
0,2
0,1
0
MR+/-
MR-/-
MR+/-
MR-/-
P0
P4

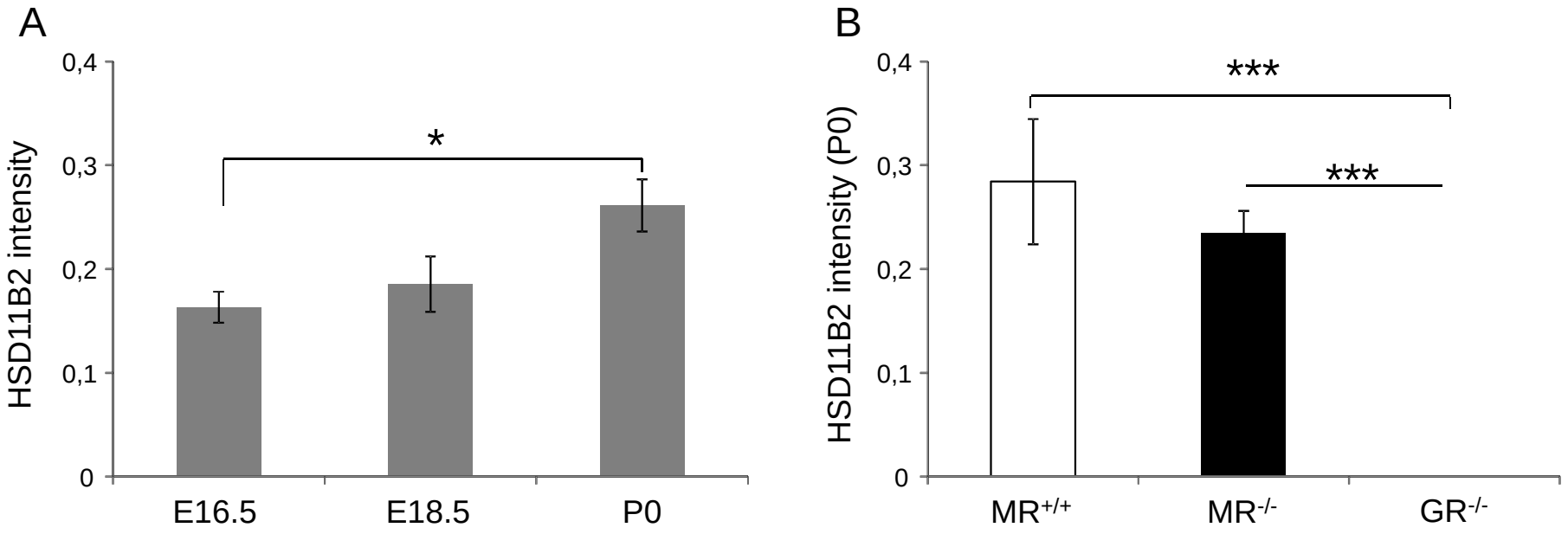
A
HSD11B2 intensity
0,4
0,3
0,2
0,1
0
*
E16.5
E18.5
P0
B
HSD11B2 intensity (P0)
0,4
0,3
0,2
0,1
0
***
***
MR+/+
MR-/-
GR-/-

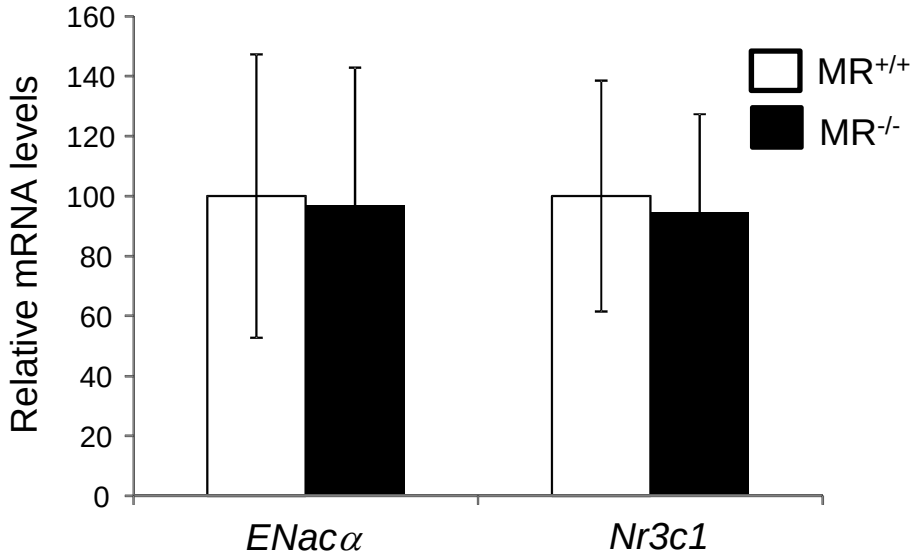
160
140
120
100
80
60
40
20
0
Relative mRNA levels
MR+/+
MR-/-
ENacα
Nr3c1

Supplementary Information

Supplementary Materials and Methods

Ethics Statement and Animal Experimentation

All mice were handled in accordance with the current Spanish and European regulations, and approved by our institution's Ethics committee (approval ID for project SAF2011-28115).

For analysis of MR expression during development, mice were subjected to timed matings, and embryo skin samples were obtained by cesarean derivation. At least 3 samples of dorsal WT (B6D2 mice, Janvier Labs) skin for each time-point (E15.5, E16.5, E18.5, P0, 5-wk, and 8-wk) or $MR^{+/+}$, $MR^{+/-}$ and $MR^{-/-}$ (P0) were analyzed for RNA and protein expression.

$MR^{-/-}$ mice were generated using a strategy based on generalized CRE-mediated recombination of $MR^{loxP/loxP}$ mice. This approach relies on the fact that the keratinocyte-specific promoter keratin (K)5 is transcriptionally active in murine oocytes. This implies that when a female expresses CRE under the control of the K5 promoter, loxP flanked sequences will be deleted in all tissues of the offspring, even in littermates that do not inherit the CRE allele (s7). This strategy has been successfully used to achieve ubiquitous CRE-mediated recombination (s7). Consequently, by intercrosses of K5-$Cre^{+/-}$//$MR^{loxP/+}$ females and 0Cre//$MR^{loxP/+}$ males, three different genotypes were obtained: $MR^{+/+}$, $MR^{+/-}$ and $MR^{-/-}$ mice. $MR^{+/+}$ and $MR^{+/-}$ mice were used as controls as the phenotype of their skin was indistinguishable.

Histological and Immunohistochemical analysis

Dorsal skin samples from litters of $MR^{+/-}$ and $MR^{-/-}$ mice at E17.5 (n= 22), P0 (n= 33), or P4 (n= 12) were collected, fixed in 70% ethanol and embedded in paraffin. BrdU incorporation was assessed by immunohistochemistry (anti-BrdU, biotest, Roche, Indianapolis, IN) in paraffin-embedded sections from mice injected with BrdU 1 hr prior to sacrifice (130 μg/g of body weight, Roche). Polyclonal antibodies to K5 (PRB-160P), K10 (PRB-159P), and loricrin (PRB-145P) were from Covance (Babco, Berkeley, CA). HSD11B2 antibody was from Santa Cruz (sc-20176). Secondary biotin-conjugated anti-rabbit or anti-mouse antibodies (Jackson ImmunoResearch) were used. At least 4 skin samples of each genotype and age (E16.5, E18.5, and P0 WT; and P0 $MR^{+/+}$, $MR^{-/-}$ and $GR^{-/-}$) were used for histopathological analysis.

For lipid staining, sections (P0 and P4 $MR^{+/-}$ and $MR^{-/-}$ mice, n= 3 per genotype) were incubated with 1mg ml^{-1} Nile Red (Sigma) in phosphate-buffered saline along with 4´-6-diamidino-2-phenylindole for 5 minutes at room temperature (8).

Epidermal dye permeability assay was performed with 1% toluidine blue dye (Sigma) as described (s14) in at least five individuals of each genotype ($MR^{+/+}$, $MR^{+/-}$ and $MR^{-/-}$).

Morphometrical analysis and immunohistochemistry quantitation

Morphometrical analysis and quantitation of immunohistochemical staining was performed using the software IMAGE-PRO PLUS 6.0 (Media Cybernetics, Silver Spring, MD, USA). For each sample, five microphotographs were taken at 100x magnification following a method of semi-randomization, which excluded altered zones. A Leica DM1000 microscope, a Leica EC3 camera and Leica LAS EZ software (Leica Microsystems, Wetzlar, Germany) were used.

The epidermal thickness was determined in H&E stained skin sections of $MR^{+/-}$ and $MR^{-/-}$ E17.5, P0 and P4 mice (at least n= 6 per genotype). At least 5 images and 10 sections were used per sample. For quantitation of K5, K10, and LOR staining (Fig. 1G), we determined the percentage of epidermal thickness that was positive for each marker by manually measuring the area. For that purpose, 10 semi-randomized measurements of marker-positive epidermis were taken in each image. Additionally, for LOR and HSD11B2 staining (Fig. S2B, S3), the intensity of each marker was quantitated by selecting the corresponding expression in each image, and measuring the mean intensity of pixels within the segmented in the microphotograph. Average intensity of expression of each marker was calculated as mean of all images and expressed as relative intensity units.

RNA isolation and Quantitative RT-PCR

RNA was isolated from mouse dorsal epidermis using Trizol (Invitrogen, Molecular Probes, Eugene, Oregon) and reverse transcribed using oligo-dT and RevertAid H-minus Reverse Transcriptase (Fermentas Inc., Burlington, Canada). Quantitative PCR was conducted using specific oligonucleotides and FastStart Universal SYBR Green Master ROX (Roche) in an Applied Biosystems 7500 Fast real time PCR system. Data were normalized to *Hprt1* expression. Specific primers used were as follows: 5´- TGCTATGCTTTGCTCCTGATCTG-3´, 5´-TGTCAGTTGATAAAACCGCTGCC-3´ for *Nr3c1*; 5´-GTGGACAGTCCTTTCACTACCG-3´, 5´-TGACACCCAGAAGCCTCATCTC-3´ for *Nr3c2*; 5´-CTAATGATGCTGGACCACACC-3´, 5´-AAAGCGTCTGCTCCGTGATGC-3´ for *ENacα*; 5´-GGAGCCGCACTTATCTGAA-3´, 5´-GACCTGGCAGTCAATACCA-3´ for *Hsd11b1*; 5´-CTGCAGATGGATCTGACCAA-3´, 5´-GTCAGCTCAAGTGCACCAAA-3´ for *Hsd11b2*; 5´-GAGCAAAGATGAGGCTGAGG-3´, 5´-CCTCCGCATCAGAAATCAAT-3´ for *Krt77*; 5´-TGGTACTCAAGGCCGAGA-3´, 5´-TTTGTCCTGATGACTGCTGAAGAC-3´ for *Sprr2d*; and 5´-TCAGTCAACGGGGGACATAAA-3´, 5´-GGGGCTGTACTGCTTAACCAG -3´ for *Hprt1*.

Immunoblotting

Preparation of whole cell extracts and immunoblotting were performed as described (7). Polyclonal antibody against MR was from Abcam (ab64457; Bristol, UK) and anti-actin was from Sigma (A2066). Secondary peroxidase-conjugated anti-rabbit antibody (Amersham) was used.

Supplementary Figures

Supplementary Fig. 1. Relative mRNA levels of *Nr3c1*, *Krt77*, and *Sprr2d* in embryonic (E15.5-E18.5) and newborn (P0) mouse skin. Statistically significant differences relative to E15.5 are indicated (n= 4 per age; * $p<0.05$, ** $p<0.01$, *** $p<0.001$).

Supplementary Fig. 2. Quantitation of epidermal thickness (A) and loricrin immunostaining (B) in $MR^{+/-}$ and $MR^{-/-}$ P0 and P4 mice (n= 6 per genotype). The intensity of immunostaining for loricrin is expressed as relative intensity units. No statistically significant changes were found.

Supplementary Fig. 3. Quantitation of epidermal HSD11B2 immunostaining A. Comparison between embryonic (E16.5, E18.5) and newborn (P0) epidermis (n= 4 per age; * $p<0.05$). B. Epidermal staining intensity in P0 $MR^{+/+}$, $MR^{-/-}$, and $GR^{-/-}$ mice P0 (n= 4 per genotype; *** $p<0.001$). Data are expressed as relative intensity units.

Supplementary Fig. 4. Relative mRNA levels of the α-subunit of the amiloride-sensitive epithelial Na channel (*ENaCα*/*Scnn1a*) and *Nr3c1* in $MR^{-/-}$ *vs* $MR^{+/+}$ P0 skin (n= 5 per genotype).

Supplementary References

s1 Schmuth M, Watson RE, Deplewski D, Dubrac S, Zouboulis CC & Grifiths CE 2007 Nuclear hormone receptors in human skin. *Hormone Metabolism Research* **39**:96–105.

s2 Slominski A & Wortsman J 2000 Neuroendocrinology of the skin. *Endocrine Rev* **21**:457–487.

s3 Slominski A, Wortsman J, Tuckey RC & Paus R 2007 Differential expression of HPA axis homolog in the skin. *Mol Cell Endocrinol* **265-266**:143–149.

s4 Bayo P, Sanchis A, Bravo A, Cascallana JL, Buder K, Tuckermann J, Schütz G & Pérez P 2008 Glucocorticoid receptor is required for skin barrier competence. *Endocrinology* **149**(3):1377–1388.

s5 Sainte Marie Y, Toulon A, Paus R, Maubec E, Cherfa A, Grossin M, Descamps V, Clemessy M, Gasc JM, Peuchmaur M, Glick A, Farman N & Jaisser F 2007 Targeted Skin Overexpression of the Mineralocorticoid Receptor in Mice Causes Epidermal Atrophy, Premature Skin Barrier Formation, Eye Abnormalities, and Alopecia. *American Journal of Pathology* **171**:846–860.

s6 Pérez P, Page A, Bravo A, del Río M, Gimenez-Conti I, Budunova I, Slaga TJ & Jorcano JL 2001 Altered skin development and impaired proliferative and inflammatory responses in transgenic mice overexpressing the glucocorticoid receptor. *FASEB Journal* **15**:2030–2036.

s7 Ramirez A, Page A, Gandarillas A Zanet J, Pibre S, Vidal M, Tusell L, Genesca A, Whitaker DA, Melton DW & Jorcano JL 2004 A keratin K5Cre transgenic line appropriate for tissue–specific or generalized Cre–mediated recombination. *Genesis* **39**:52–7

s8 Berger S, Wolfer DP, Selbach O, Alter H, Erdmann G, Reichardt HM, Chepkova AN, Welzl H, Haas HL, Lipp HP & Schütz G 2006 Loss of the limbic mineralocorticoid receptor impairs behavioral plasticity. *Proc Natl Acad Sci USA* **103**(1):195–200.

s9 Berger S, Bleich M, Schmid W, Cole TJ, Peters J, Watanabe H, Kriz W, Warth R, Greger R & Schütz G 1998 Mineralocorticoid receptor knockout mice: pathophysiology of Na+ metabolism. *Proc Natl Acad Sci USA* **95**(16):9424–9429.

s10 Charles RP, Guitard M, Leyvraz C, Breiden B, Haftek M, Haftek-Terreau Z, Stehle JC, Sandhoff K & Hummler E 2008 Postnatal requirement of the epithelial sodium channel for maintenance of epidermal barrier function. *J Biol Chem* **283**(5):2622–30.

s11 Schulz-Baldes A, Berger S, Grahammer F, Warth R, Goldschmidt ·I, Peters J,·Schütz G, Greger R & Bleich M 2001 Induction of the epithelial Na+ channel via glucocorticoids in mineralocorticoid receptor knockout mice. *Pflügers Arch - Eur J Physiol* **443**:297–305.

s12 Stojadinovic O, Lee B, Vouthounis C, Vukelic S, Pastar I, Blumenberg M, Brem H & Tomic-Canic M 2007 Novel genomic effects of glucocorticoids in epidermal keratinocytes. *J Biol Chem* **282**:4021–4034.

s13 Reichardt HM & Schutz G 1996 Feedback Control of Glucocorticoid Production is Established during Fetal Development *Mol Medicine* **2**(6):735–744.

s14 Byrne C, Avilion AA, O'Shaughnessy RF, Welti JC & Hardman MJ 2010 Whole-mount assays for gene induction and barrier formation in the developing epidermis. *Methods Mol Biol* **585**:271–86.